

# Effect of Graphene Fermi Level on the Raman Scattering Intensity of Molecules on Graphene

Hua Xu,<sup>†,‡</sup> Liming Xie,<sup>†</sup> Haoli Zhang,<sup>‡,\*</sup> and Jin Zhang<sup>†,\*</sup>

<sup>†</sup>Center for Nanochemistry, Beijing National Laboratory for Molecular Sciences, Key Laboratory for the Physics and Chemistry of Nanodevices, State Key Laboratory for Structural Chemistry of Unstable and Stable Species, College of Chemistry and Molecular Engineering, Peking University, Beijing 100871, China, and <sup>‡</sup>State Key Laboratory of Applied Organic Chemistry, College of Chemistry and Chemical Engineering, Lanzhou University, Lanzhou 730000, China

Surface-enhanced Raman scattering (SERS) was discovered more than three decades ago and has been widely utilized since then.<sup>1,2</sup> Despite numerous experimental and theoretical works focusing on the origin of SERS, there remain many controversies about its mechanism.<sup>3,4</sup> It is generally agreed that there are two contributors to SERS intensities: an electromagnetic mechanism (EM) and a chemical mechanism.<sup>5</sup> Much more work has been focused on the former mechanism and has advanced the understanding.<sup>6</sup> However, compared to the extensive study of the EM mechanism, study of the chemical mechanism is still scarce. Generally, the photoinduced metal–molecule charge transfer (CT) is believed to be the mechanism responsible for chemical enhancement in SERS, yet its microscopic mechanism and relative importance are still hotly debated.<sup>7</sup> A key obstacle to studying the CT mechanism is the fact that the two mechanisms occur simultaneously in the traditional metal substrate SERS.<sup>3,8</sup> To date, no reliable experimental strategy appears to have been developed to isolate and quantify these effects.<sup>6</sup>

On the basis of the characteristics of CT, there are two basic requirements: one is direct contact between the probe molecule and the substrate, and the CT process occurs only for the first layer of molecules on the SERS substrate (first layer effect) because it is a short-range effect. The other is the energy alignment between the molecular energy level (HOMO, LUMO) of the molecules and the Fermi level of the metal substrate.<sup>9,10</sup> Therefore, tuning the position of the Fermi level of metal using an external voltage source can, in principle, drive the entire system in and out of CT resonance.<sup>9</sup> This approach was extensively employed in the past to study the CT resonance contribution

**ABSTRACT** We studied the modulation of Raman scattering intensities of molecules on graphene by tuning the graphene Fermi level with electrical field effect (EFE). A series of metal phthalocyanine (M-Pc) molecules (M = Mn, Fe, Co, Ni, Cu, Zn), which have different molecular energy levels, were used as probe molecules. The Raman intensities of all these M-Pc molecules become weaker when the graphene Fermi level is up-shifted by applying a positive gate voltage, while they become stronger when the graphene Fermi level is down-shifted by applying a negative gate voltage. However, this Raman intensity modulation only occurs when applying the gate voltage with a fast sweep rate, while it is nearly absent when applying the gate voltage with a slow sweep rate, which is likely due to the arising of the hysteresis effect in the graphene EFE. In addition, the Raman modulation ability for M-Pc molecules with smaller energy gaps is larger than that with larger energy gaps due to the difference in the energy alignment between graphene and these M-Pc molecules. Furthermore, this modulation shows the greatest one on single-layer graphene and mainly comes from the first layer of molecules which are in direct contact with graphene. The Raman modulation of molecules in GERS with the EFE suggests that the Raman enhancement for GERS occurs through a chemical enhancement mechanism.

**KEYWORDS:** graphene Fermi level · chemical enhancement · electric field modulation

by examining the dependence of SERS of molecules on electrochemical potential.<sup>5,9–12</sup> However, because these experiments were usually carried out on metal electrodes, many hot spots as well as areas with the large EM enhancement will inevitably contribute to the total Raman signal.<sup>5</sup>

Graphene, a semimetal with a zero band gap, shows many novel physical and chemical properties for its unique electronic structure.<sup>13</sup> Our previous work has shown that graphene can be used as a substrate to suppress fluorescence<sup>14</sup> and enhance Raman signals of molecules.<sup>15</sup> We call this Raman enhancement technique graphene-enhanced Raman scattering (GERS). The graphene surface is relatively smooth despite fluctuations arising from the underlying substrate.<sup>16</sup> Also, optical transmission through the graphene surface in the visible range is greater

\* Address correspondence to haoli.zhang@lzu.edu.cn, jinzhang@pku.edu.cn.

Received for review September 1, 2010 and accepted June 16, 2011.

Published online June 16, 2011  
10.1021/nn103237x

© 2011 American Chemical Society

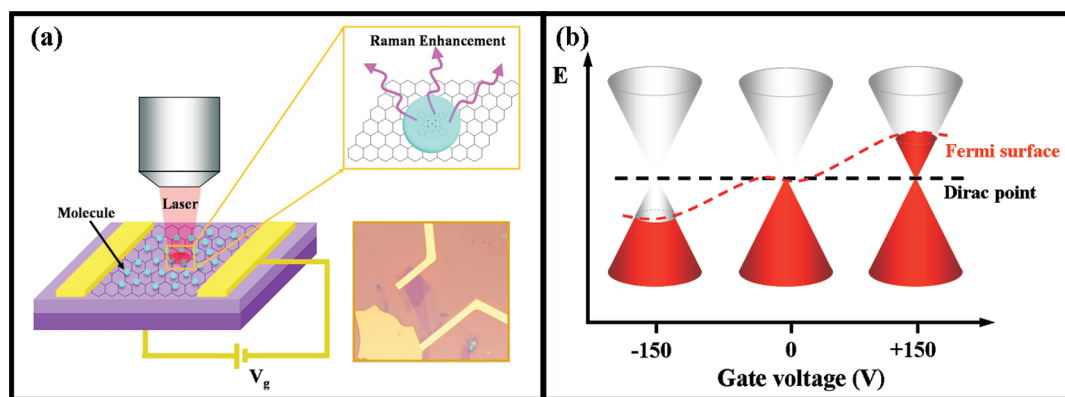


Figure 1. (a) Schematic diagram of the experiment setup and an optical image of the graphene device. (b) Fermi level variation of single-layer graphene modulated with electrical field.

than 95%.<sup>17,18</sup> Furthermore, the surface plasmon on graphene is in the range of terahertz rather than in visible range.<sup>19</sup> On the basis of these considerations, we think that the GERS mechanism cannot be EM and therefore attribute it to CT. So, GERS provides an excellent opportunity to study CT separately from EM.

Here, we demonstrate an electrical field modulation experimental strategy to study the effect of graphene Fermi level variation on the Raman scattering intensities of molecules on graphene. The approach is based on modulating the energy alignment between the energy level of the molecule and the Fermi level of graphene using the benefit that the Fermi level of graphene can be modulated with an electrical field effect (EFE)<sup>20,21</sup> to modulate the CT between the graphene and the molecules. Figure 1a shows a schematic diagram of the *in situ* Raman measurement with the electric field-induced graphene Fermi level modulation, and we use a series of M-Pc molecules as probe molecules to study the effect of the molecular energy level on the Raman intensity modulation; these M-Pc molecules have similar molecular structures but different energy levels (see Supporting Information Figure S1). We find that the Raman intensities of all these M-Pc molecules show modulation with the EFE, and the modulation ability is related to the energy level of these M-Pc molecules. In addition, the Raman modulation is affected by the gate voltage sweep rate, which is likely due to the arising of hysteresis effect in graphene EFE. This EFE modulation of GERS spectra proves that the Raman enhancement mechanism of GERS works *via* chemical enhancement.

## RESULTS AND DISCUSSION

To investigate whether the Raman intensities of molecules in GERS can be modulated with an EFE, we first study the EFE modulation of the graphene Fermi level using the *in situ* Raman spectroscopy. We focus on the doubly degenerate optical phonon of  $E_{2g}$  symmetry at  $1580\text{ cm}^{-1}$ , known as the G band. Our Raman spectra data demonstrate that the frequency

and full width at half-maximum (fwhm) of the G band and the intensity ratio of the 2D ( $\sim 2700\text{ cm}^{-1}$ ) and G bands  $A(2D)/A(G)$  show a linear dependence on the EFE (see Supporting Information Figure S2), which is similar to the results in previous work.<sup>20,22–24</sup> The linear dependence of the phonon frequency, fwhm of the G band, and  $A(2D)/A(G)$  on the EFE are attributed to the modulation of the graphene Fermi level with the electric field.<sup>20</sup> Figure 1b shows a schematic diagram of the graphene Fermi level variation modulated with the EFE. For intrinsic single-layer graphene, the positions of the Fermi level and Dirac point are equal.<sup>25</sup> However, when applying a negative (positive) gate voltage, the Fermi level of graphene will shift below (above) the Dirac point due to the EFE-induced hole (electron) doping. Hence, the Fermi level of graphene can be modulated continuously by the EFE and monitored through the Raman spectra in our experiment. In the following study, we focus on the modulation of Raman intensities of molecules in GERS with an EFE.

The Raman intensity variations of Co-Pc molecules modulated by sweeping the gate voltage from  $-150$  to  $+150\text{ V}$  at intervals of 20, 50, and 150 V are shown in Figure 2a–c. Corresponding Raman intensity variations were determined by comparing the intensities of the strongest Raman peak at  $1539\text{ cm}^{-1}$ , which is assigned to the C–N–C stretching mode of the phthalocyanine macrocycle.<sup>26</sup> This mode has been found to shift by up to  $50\text{ cm}^{-1}$  depending on the metal present in the phthalocyanine macrocycle.<sup>12,26</sup> For convenient comparison, we also extract the Raman signal of the C–N–C bridge for other M-Pc molecules in the following study. Unexpectedly, the Raman intensity of Co-Pc shows nearly no modulation by sweeping the gate voltage from  $-150$  to  $+150\text{ V}$  at the interval of 20 V (Figure 2a), and it shows only a smaller modulation by sweeping the gate voltage at the interval of 50 V (Figure 2b). Surprisingly, the Raman intensity shows an obvious modulation if we sweep the gate voltage at the interval of 150 V (Figure 2c). From the observed results, we can find that the Raman modulation ability

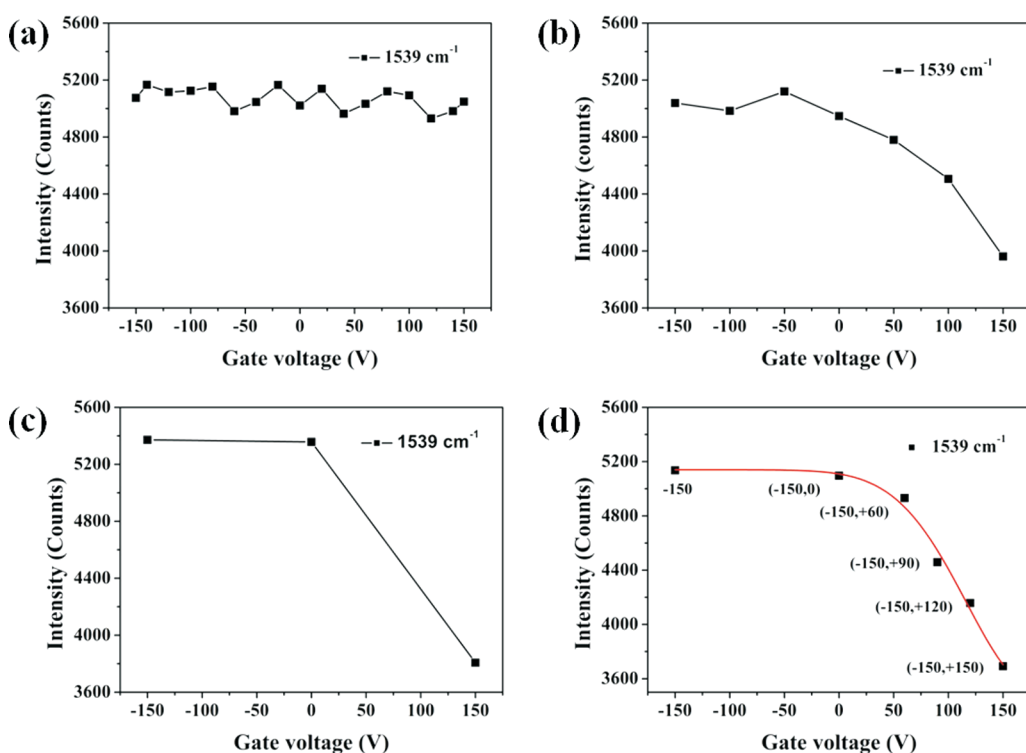


Figure 2. Plot of the GERS intensity of the 1539 cm<sup>-1</sup> band of Co-Pc extracted from the spectra which are measured by sweeping the gate voltage from -150 to +150 V with intervals of (a) 20 V, (b) 50 V, and (c) 150 V. (d) Statistics of the intensity variation of the 1539 cm<sup>-1</sup> mode modulated with different gate voltage variation spans. The plots in (d) are the corresponding intensities at gate voltages of -150, 0, +60, +90, +120, and +150 V during each gate voltage variation span.

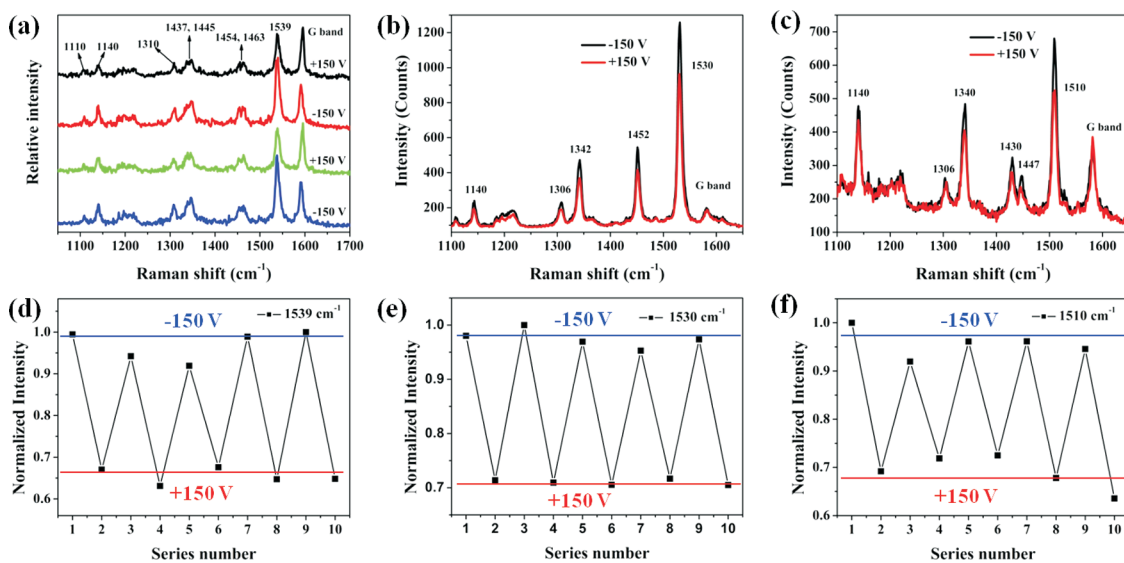
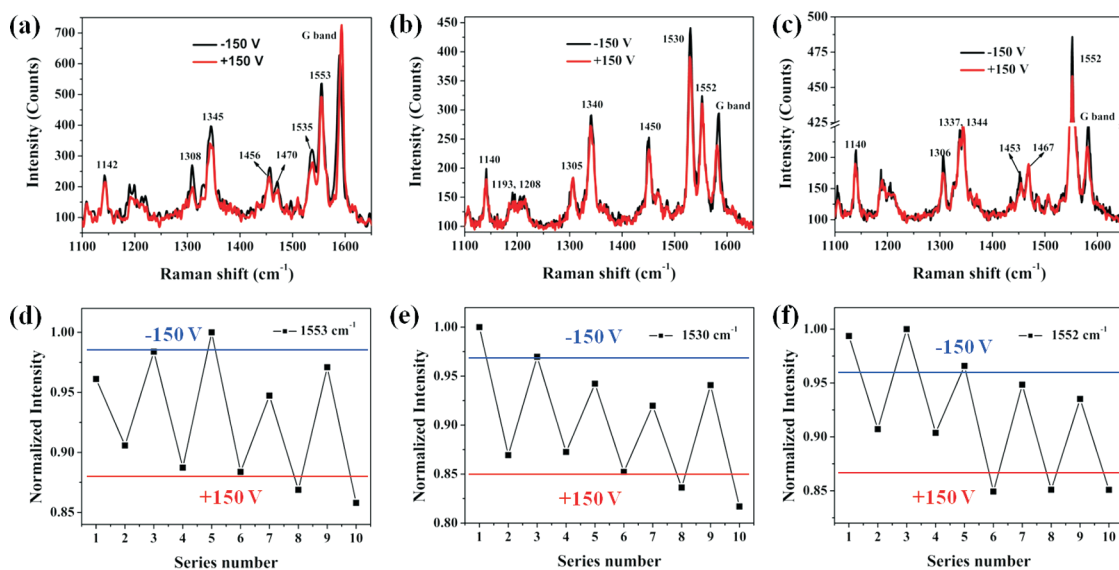


Figure 3. GERS spectra of (a) Co-Pc, (b) Cu-Pc, and (c) Zn-Pc molecules modulated with gate voltage between -150 V and +150 V. (d-f) Corresponding Raman intensity variations of the C-N-C bridge vibration mode for the Co-Pc, Cu-Pc, and Zn-Pc molecules, respectively. The intensities are normalized to the maximum value observed in the investigated gate voltage range.

is increasing with the gate voltage sweep rate increasing. The reason for this gate voltage sweep rate dependence of Raman modulation will be discussed below. Figure 2d displays the Raman intensity modulation during different gate voltage sweep spans. The Raman modulation ability is increasing with the gate voltage span increasing, which is because the modulation

window of the graphene Fermi level is enlarging with the gate voltage span increasing. However, the gate voltage applied on our graphene device cannot be larger than 150 V due to the problem of leakage currents.

Why does the Raman intensity modulation show an obvious difference modulated during the same gate voltage span but different sweep rates? From the study



**Figure 4.** GERS spectra of (a) Mn-Pc, (b) Fe-Pc, and (c) Ni-Pc molecules modulated with gate voltage between  $-150$  and  $+150$  V. (d–f) Corresponding Raman intensity variations of the C–N–C bridge vibration mode for the Mn-Pc, Fe-Pc, and Ni-Pc molecules, respectively. The intensities are normalized to the maximum value observed in the investigated gate voltage range.

on the electrical field modulation of graphene Raman spectra, we find that the frequency shift of the G band shows a hysteresis behavior, especially at a slower gate voltage sweep rate (see Supporting Information, Figure S3). As we know, the hysteresis effect is a common problem in graphene EFE, which hinders the modulation of the graphene Fermi level with electrical field, especially in a large range or at a slow gate voltage sweep rate.<sup>27</sup> So, the gate voltage sweep rate dependence of the Raman modulation in GERS is likely due to the arising of hysteresis effect in graphene EFE. From the above analysis, we know that the Raman intensity modulation with EFE will be seriously hindered due to the arising of large hysteresis effects at the slow gate voltage sweep rate. For this reason, in order to reduce the effect of hysteresis on the Raman modulation of molecules in GERS, we applied a gate voltage with a fast sweep rate in the following study.

Figure 3a–c shows the EFE-modulated GERS spectra of Co-Pc, Cu-Pc, and Zn-Pc molecules which have small energy gaps. It can be seen that the Raman signals of all these three M-Pc molecules show similar modulation behavior, the Raman scattering intensities get weaker when the graphene Fermi level is up-shifted by sweeping the gate voltage to  $+150$  V, while they get stronger when the graphene Fermi level is down-shifted by sweeping the gate voltage to  $-150$  V. This modulation is reversible as shown in Supporting Information Figure S4. In order to compare the difference in the Raman modulation between different M-Pc molecules, the Raman intensity variation of the C–N–C bridge vibration mode of Co-Pc, Cu-Pc, and Zn-Pc molecules under the EFE modulation is normalized as shown in Figure 3d–f. As seen from the figures, the Raman modulation percentage for Co-Pc, Cu-Pc,

**TABLE 1.** Energy Gap and Raman Modulation Percentage of Different M-Pc Molecules<sup>a</sup>

M-Pc molecules	Mn-Pc	Fe-Pc	Ni-Pc	Co-Pc	Cu-Pc	Zn-Pc
energy gap (eV)	3.14	2.60	3.20	1.61	1.70	1.94
Raman modulation percentage (%)	12.3	10.5	9.4	34.2	29.7	30.3

<sup>a</sup> The Raman modulation percentage is obtained from the intensity variation of the C–N–C bridge vibration mode of these M-Pc molecules modulated with the gate voltage sweep between  $-150$  and  $+150$  V.

and Zn-Pc molecules can up to 34.2, 29.7, and 30.3%, respectively.

The EFE-modulated GERS spectra of Mn-Pc, Fe-Pc, and Ni-Pc molecules, which have large energy gaps, are shown in Figure 4a–c. The Raman signals of Mn-Pc, Fe-Pc, and Ni-Pc molecules show a similar modulation trend as those for Co-Pc, Cu-Pc, and Zn-Pc molecules. The Raman intensities of these three M-Pc molecules get weaker as the gate voltage sweeps to  $+150$  V, while they get stronger as gate voltage sweeps to  $-150$  V, and they also show reversible modulations. However, compared to the relative larger Raman modulations for Co-Pc, Cu-Pc, and Zn-Pc molecules, the Raman modulations for Mn-Pc, Fe-Pc, and Ni-Pc molecules are relatively smaller. From the normalized Raman intensity variation of the C–N–C bridge vibration mode of Mn-Pc, Fe-Pc, and Ni-Pc molecules (Figure 4d–f), we can see that the Raman modulation percentages for these molecules can only reach 12.3, 10.5, and 9.4%, respectively.

Table 1 shows the molecular energy gaps and the Raman modulation percentages of these different M-Pc molecules. It can be found that the Raman scattering intensities for molecules with small energy gaps (Co-Pc, Cu-Pc, and Zn-Pc) show more obvious modulation than those for molecules with large energy gaps

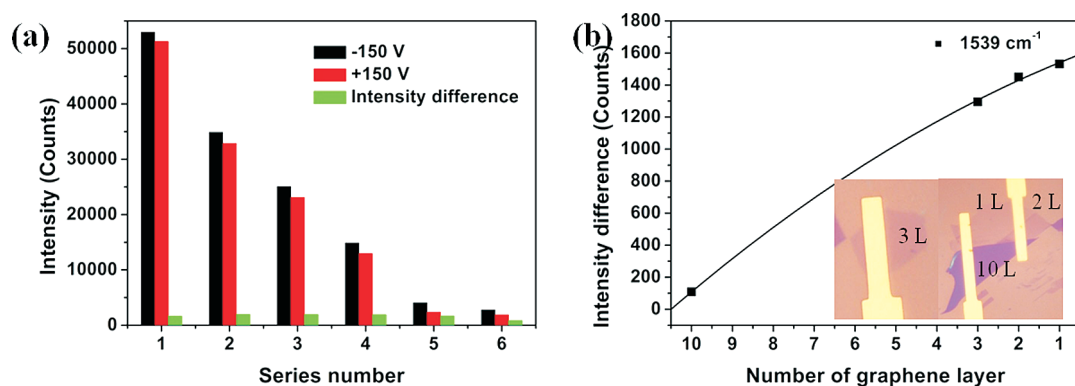


Figure 5. GERS intensity variation of the  $1539\text{ cm}^{-1}$  band of Co-Pc molecules, which were adsorbed (a) with different amounts and (b) on different graphene layers, modulated with the gate voltage between  $-150$  and  $+150\text{ V}$ . The amount of molecules on the sample decreases with an increase in iteration number from 1 to 6 in (a) by sequential washing with solvent.

(Mn-Pc, Fe-Pc, and Ni-Pc). This is because these M-Pc molecules have a different molecular energy level, which leads the energy alignment between the graphene Fermi level and the molecular energy level of these M-Pc molecules to be different. Therefore, the Raman modulation of molecules in GERS is affected by not only the position of graphene Fermi level but also the positions of the energy level of the probe molecule. In addition, a frequency shift from the comparison of the Raman spectra of the M-Pc adsorbed on graphene and those of M-Pc powder is observed (see Supporting Information Figure S5). This frequency shift is attributed to the results of the CT between graphene and M-Pc.<sup>28,29</sup>

As studied in our previous work about the “first layer effect”, the CT process in GERS was strongly related to the distance between the graphene substrate and the molecules, and the CT only occurred at the first layer of molecules.<sup>30</sup> So, electric field modulation of the Raman signals in our GERS system should also act on the first layer of molecules. We studied the effect of the amount of molecules adsorbed on graphene on the EFE modulation of GERS spectra. The experimental details are shown in the Supporting Information Part II. Briefly, the amount of molecules adsorbed on graphene surface gradually decreases from measurements 1 to 6 in Figure 5a by sequential washing with solvent. We can see that the Raman intensity of Co-Pc decreases as the amount of molecules on graphene decreases from measurements 1 to 6. However, the intensity difference of the Raman signal modulated by the gate voltage does not change greatly for measurements from 1 to 5. However, the intensity difference shows an obvious decrease at the sixth measurement, which is because the amount of molecules adsorbed on graphene has decreased to less than one layer. The results suggest that the Raman modulation predominantly comes from the first layer of molecules that are in direct contact with graphene.

We also studied the effect of the number of graphene layers on the EFE modulation of the GERS spectra. As shown in Figure 5b, the intensity difference of the

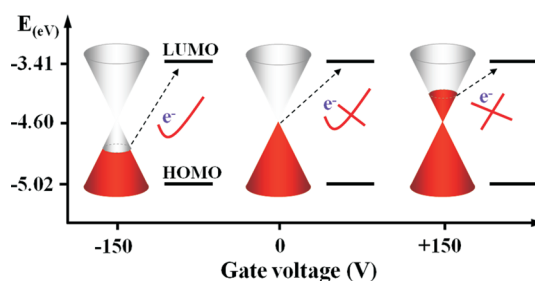


Figure 6. Schematic representation of the effect of the energy level alignment between the molecular energy level and graphene Fermi level on the charge transfer resonance.

Raman signal of Co-Pc modulated by a sweeping gate voltage between  $-150$  and  $+150\text{ V}$  increases as the number of graphene layers increases, and the largest modulation occurs on the single-layer graphene. Previous studies have shown that the modulation ability of the graphene Fermi level with EFE decreases as the number of the graphene layers increases due to the screening effect.<sup>31,32</sup> Thereby, the Raman intensity modulation ability of molecules in GERS shows a decrease as the graphene layer number increases.

In view of all of the above results and discussions about the EFE modulation of the GERS spectra, we consider that the mechanism of GERS should be the CT enhancement. On the basis of the characteristic of the CT and the data from our work, an energy diagram for the adsorbed complexes is presented to illustrate how the graphene Fermi level variation affects the Raman intensities of molecules in GERS. We take Co-Pc molecules as an example to analyze this relationship in Figure 6. The HOMO and LUMO of Co-Pc are at  $-5.02$  and  $-3.41\text{ eV}$ ,<sup>33</sup> respectively, and the Fermi level of intrinsic graphene is about  $-4.6\text{ eV}$ <sup>21</sup> if we assume that the vacuum level is set to zero here. Although the accurate position of graphene Fermi level under the positive and negative gate voltage cannot be determined due to the hysteresis effect, we can make sure that the graphene Fermi level can be up-shifted by applying a positive gate voltage, while it can be down-shifted by

applying a negative gate voltage. So, the energy gap between the LUMO of the Co-Pc molecule and the Fermi level of graphene is about 1.19 eV at the gate voltage of 0 V, which is slightly smaller than the energy of the laser (1.96 eV for 632.8 nm laser source). In this case, the Raman intensities of the molecules can be enhanced because the CT resonance is very broad,<sup>5</sup> and the CT resonance process is greatly enhanced when applying a negative gate voltage to down-shift the graphene Fermi level because that makes the energy gap even closer to the energy of the laser. The CT resonance process is hindered when applying a positive gate voltage to up-shift the graphene Fermi level because that makes the energy gap far away from the energy of the laser. Therefore, the Raman intensities of molecules in GERS get stronger by applying a negative gate voltage, while they get weaker by applying a positive gate voltage.

## CONCLUSIONS

In this work, we have investigated the modulation of the Raman scattering intensities of molecules in GERS

by tuning the graphene Fermi level with an EFE. The Raman intensities all of the M-Pc molecules get weaker as the graphene Fermi level up-shifts by applying a positive gate voltage, while they get stronger as the graphene Fermi level down-shifts by applying a negative gate voltage. However, the Raman modulation percentage of M-Pc molecules with small energy gaps is larger than that of M-Pc molecules with large energy gaps, which is likely due to the difference in the energy alignment between the Fermi level of graphene and the molecular energy level of these M-Pc molecules. Furthermore, such Raman modulations predominantly come from the first layer of molecules in direct contact with the graphene and significantly reduce with the graphene layer number increasing. All of these observed results suggest that the enhanced Raman scattering of molecules on graphene is due to the CT resonance mechanism, and the resonance conditions can be modulated by changing the Fermi level of graphene. This approach will benefit the study of the basic properties of CT enhancement separately from the EM enhancement in the future.

## METHODS

**Preparation of Graphene Devices.** Graphene was prepared by mechanical exfoliation of kish graphite (Covalent Materials Corp.) using Scotch tape on Si wafers covered with 300 nm thick SiO<sub>2</sub>. Graphene thickness was characterized by optical microscopy (OM) and Raman spectroscopy. Electrical contacts with graphene were made by standard electron-beam lithography and electron-beam evaporation of Cr (5 nm) and Au (50 nm). The doped Si substrate was used as the gate electrode, and the oxide served as the dielectric.

**Deposition Molecules on Graphene Devices.** We deposited organic molecules on the surface of graphene by simply soaking the SiO<sub>2</sub>/Si substrate with graphene in the solution of the molecules. All of these M-Pc molecules were dissolved in *N,N*-dimethylformamide (DMF) with a concentration of  $1 \times 10^{-6}$  M. The soaking time was 1 h for all of the molecular solutions. After soaking, the samples were washed with DMF to remove any free molecules and then dried under N<sub>2</sub>.

**In Situ Raman Measurement and Electric Field-Induced Graphene Fermi Level Modulation.** Raman spectra were obtained *in situ* at each gate voltage using a Horiba HR800 Raman system equipped with a homemade probe station. A 632.8 nm line from a He–Ne laser was used as the excitation laser. The spectrum integration time was 10 s per spectrum. The incident laser beam was focused by a 50 $\times$  objective, and the laser power on the samples was kept below 0.5 mW to avoid laser-induced heating. The intensities and frequencies of the peaks were obtained by fitting them with a Lorentzian function.

**Acknowledgment.** This work was supported by NSFC (50972001, 20725307, and 50821061), MOST (2011CB932601, 2007CB936203), and “the Fundamental Research Funds for the Central Universities”. We thank B.H. Peng, X. Ling, and W.G. Xu for their useful discussion.

**Supporting Information Available:** Additional figures showing the molecular structures and the relative energy levels of these M-Pc molecules, Raman spectra modulation of graphene with EFE, hysteresis effect in graphene EFE, reversible Raman modulation of Co-Pc with EFE, comparison of the GERS spectra of M-Pc and the spectra of its powder, and experimental details of studying the effect of molecule amount on GERS modulation.

This material is available free of charge via the Internet at <http://pubs.acs.org>.

## REFERENCES AND NOTES

- Morton, S. M.; Jensen, L. Understanding the Molecule–Surface Chemical Coupling in SERS. *J. Am. Chem. Soc.* **2009**, *131*, 4090–4098.
- Li, J. F.; Huang, Y. F.; Ding, Y.; Yang, Z. L.; Li, S. B.; Zhou, X. S.; Fan, F. R.; Zhang, W.; Zhou, Z. Y.; Wu, D. Y.; *et al.* Shell-Isolated Nanoparticle-Enhanced Raman Spectroscopy. *Nature* **2010**, *464*, 392–395.
- Campion, A.; Kambhampati, P. Surface-Enhanced Raman Scattering. *Chem. Soc. Rev.* **1998**, *27*, 241–250.
- Haynes, C. L.; McFarland, A. D.; Duyn, R. P. V. Surface-Enhanced Raman Spectroscopy. *Anal. Chem.* **2005**, *77*, 338–346.
- Shegai, T.; Vaskevich, A.; Rubinstein, I.; Haran, G. Raman Spectroelectrochemistry of Molecules Individual Electro-magnetic Hot Spots. *J. Am. Chem. Soc.* **2009**, *131*, 14390–14398.
- Maitani, M. M.; Ohlberg, D. A. A.; Li, Z.; Allara, D. L.; Stewart, D. R.; Williams, R. S. Study of SERS Chemical Enhancement Factors Using Buffer Layer Assisted Growth of Metal Nanoparticles on Self-Assembled Monolayers. *J. Am. Chem. Soc.* **2009**, *131*, 6310.
- Park, W.-H.; Kim, Z. H. Charge Transfer Enhancement in the SERS of a Single Molecule. *Nano Lett.* **2010**, *10*, 4040–4048.
- Sánchez-Cortés, S.; García-Ramos, J. V., Surface-Enhanced Raman of 1,5-Dimethylcytosine Adsorbed on a Silver Electrode and Different Metal Colloids: Effect of Charge Transfer Mechanism. *Langmuir* **16**, 764–770.
- Osawa, M.; Matsuda, N.; Yoshii, K.; Uchida, I. Charge Transfer Resonance Raman Process in Surface-Enhanced Raman Scattering from *p*-Aminothiophenol Adsorbed on Silver: Herzberg–Teller Contribution. *J. Phys. Chem.* **1994**, *98*, 12702–12707.
- Arenas, J. F.; Fernández, D. J.; Soto, J.; Tocón, I. L. p.; Otero, J. C. Role of the Electrode Potential in the Charge-Transfer Mechanism of Surface-Enhanced Raman Scattering. *J. Phys. Chem. B* **2003**, *107*, 13143–13149.

11. Corio, P.; Temperini, M. r. L. A.; Santos, P. S.; Rubim, J. C. Contribution of the Charge Transfer Mechanism to the Surface-Enhanced Raman Scattering of the Binuclear Ion Complex  $[\text{Fe}_2(\text{Bpe})(\text{CN})_{10}]^{6-}$  Adsorbed on a Silver Electrode in Different Solvents. *Langmuir* **1999**, *15*, 2500–2507.
12. Corio, P.; Rubim, J. C.; Aroca, R. Contribution of the Herzberg-Teller Mechanism to the Surface-Enhanced Raman Scattering of Iron Phthalocyanine Adsorbed on a Silver Electrode. *Langmuir* **1998**, *14*, 4162–4168.
13. Zhang, Y.; Tang, T.-T.; Girit, C.; Hao, Z.; Martin, M. C.; Zettl, A.; Crommie, M. F.; Shen, Y. R.; Wang, F. Direct Observation of a Widely Tunable Bandgap in Bilayer Graphene. *Nature* **2009**, *159*, 820–823.
14. Xie, L.; Ling, X.; Fang, Y.; Zhang, J.; Liu, Z. Graphene as a Substrate To Suppress Fluorescence in Resonance Raman Spectroscopy. *J. Am. Chem. Soc.* **2009**, *131*, 9890–9891.
15. Ling, X.; Xie, L.; Fang, Y.; Xu, H.; Zhang, H.; Kong, J.; Dresselhaus, M. S.; Zhang, J.; Liu, Z. Can Graphene Be Used as a Substrate for Raman Enhancement? *Nano Lett.* **2010**, *10*, 553–561.
16. Guinea, F.; Horovitz, B.; Doussal, P. L. Gauge Fields, Ripples and Wrinkles in Graphene Layers. *Solid State Commun.* **2009**, *149*, 1140–1143.
17. Bruna, M.; Borini, S. Optical Constants of Graphene Layers in the Visible Range. *Appl. Phys. Lett.* **2009**, *94*, 031901.
18. Li, X.; Zhu, Y.; Cai, W.; Borysiak, M.; Han, B.; Chen, D.; Piner, R. D.; Colombo, L.; Ruoff, R. S. Transfer of Large-Area Graphene Films for High-Performance Transparent Conductive Electrodes. *Nano Lett.* **2009**, *9*, 4359–4363.
19. Rana, F. Graphene Terahertz Plasmon Oscillators. *IEEE Trans. Nanotechnol.* **2008**, *7*, 91–99.
20. Yan, J.; Zhang, Y.; Kim, P.; Pinczuk, A. Electric Field Effect Tuning of Electron–Phonon Coupling in Graphene. *Phys. Rev. Lett.* **2007**, *98*, 166802-1–166802-4.
21. Yu, Y. J.; Zhao, Y.; Ryu, S.; Brus, L. E.; Kim, K. S.; Kim, P. Tuning the Graphene Work Function by Electric Field Effect. *Nano Lett.* **2009**, *9*, 3430–3434.
22. Pisana, S.; Lazzeri, M.; Casiraghi, C.; Novoselov, K. S.; Geim, A. K.; Ferrari, A. C.; Mauri, F. Breakdown of the Adiabatic Born–Oppenheimer Approximation in Graphene. *Nat. Mater.* **2007**, *6*, 198–201.
23. Malard, L. M.; Elias, D. C.; Alves, E. S.; Pimenta, M. A. Observation of Distinct Electron–Phonon Couplings in Gated Bilayer Graphene. *Phys. Rev. Lett.* **2008**, *101*, 257401-1–257401-4.
24. Das, A.; Pisana, S.; Chakraborty, B.; Piscanec, S.; Saha, S. K.; Waghmare, U. V.; Novoselov, K. S.; Krishnamurthy, H. R.; Geim, A. K.; Ferrari, A. C.; *et al.* Monitoring Dopants by Raman Scattering in an Electrochemically Top-Gated Graphene Transistor. *Nat. Nanotechnol.* **2008**, *3*, 210–215.
25. Gierz, I.; Riedl, C.; Starke, U.; Ast, C. R.; Kern, a. K. Atomic Hole Doping of Graphene. *Nano Lett.* **2008**, *8*, 4603–4607.
26. Tackley, D. R.; Dent, G.; Smith, W. E. Phthalocyanines: Structure and Vibrations. *Phys. Chem. Chem. Phys.* **2001**, *3*, 1419–1426.
27. Lafkioti, M.; Krauss, B.; Lohmann, T.; Zschieschang, U.; Klauk, H.; von Klitzing, K.; Smet, J. H. Graphene on a Hydrophobic Substrate: Doping Reduction and Hysteresis Suppression under Ambient Conditions. *Nano Lett.* **2010**, *10*, 1149–1153.
28. Joo, S.-W. Electric Field-induced Charge Transfer of  $(\text{Bu}_4\text{N})_2[\text{Ru}(\text{dcbpyH})_2^{2-}(\text{NCS})_2]$  on Gold, Silver, and Copper Electrode Surfaces Investigated by Means of Surface-Enhanced Raman Scattering. *Bull. Korean Chem. Soc.* **2007**, *28*, 1405–1409.
29. Li, C.; Imae, T. Protoporphyrin IX Zinc(II) Organization at the Air/Water Interface and Its Langmuir–Blodgett Films. *Langmuir* **2003**, *19*, 779–784.
30. Ling, X.; Zhang, J. First-Layer Effect in Graphene-Enhanced Raman Scattering. *Small* **2010**, *6*, 2020.
31. Falkovsky, L. A. Screening in Gated Bilayer Graphene. *Phys. Rev. B* **2009**, *80*, 113413-1–113413-4.
32. Avetisyan, A. A.; Partoens, B.; Peeters, F. M. Electric-Field Control of the Band Gap and Fermi Energy in Graphene Multilayers by Top and Back Gates. *Phys. Rev. B* **2009**, *80*, 195401-1–195401-11.
33. Liao, M.-S.; Scheinera, S. Electronic Structure and Bonding in Metal Phthalocyanines, Metal = Fe, Co, Ni, Cu, Zn, Mg. *J. Chem. Phys.* **2001**, *114*, 9780–9791.